# σ-HOLE TRIEL BOND COOPERATIVITY IN TRIMER COMPLEXES OF 1,4-DEDIHYDRO AZABORINE, AND 1,4-DEDIHYDRO BORAZINE

Sarah A. Mata*, Jordan Huang*, Vasilios Nezis*, Sai Parshetty*, and Rubén D. Parra†

Department of Chemistry and Biochemistry, DePaul University, Chicago, IL 60614

**Abstract**

**Dimer and trimer complexes of 1,4-dedihydro azaborine (azaborine) and 1,4-dedihydro borazine (borazine) were investigated with the ωB97XD/DGDZVP method. Attractive σ-hole triel bond interactions between properly placed adjacent molecules result in stable chain-like dimer and trimer complexes of $C_2$ symmetry. The interactions are found to be stronger in the borazine dimer (ΔE = -84.45 kcal/mol) than in the azaborine dimer (ΔE = -69.93 kcal/mol). Trimer formation brings about a cooperative enhancement in the electronic interaction energies of 28% and 12% in the borazine and azaborine complexes respectively. Cooperativity effects are also reflected in other indicators including the B···N intermolecular distances, and the B···N vibrational stretching frequencies. Further corroboration of cooperativity is given by the sizeable increases in the electron densities at the B···N bond critical points. Analyses based on the theory of atoms in molecules reveal that the noncovalent interactions are partly covalent.**

†Corresponding author: rparra1@depaul.edu *Undergraduate researchers and co-authors

Keywords: Triel bonds, σ-hole, cooperativity, azaborine, borazine.
Received: June, 23, 2025 Accepted: July 21, 2025 Revision received: July 23, 2025 Published July 23, 2025

## Introduction

The concept of intermolecular noncovalent interactions is introduced very early in undergraduate chemistry[1]. It helps explain, for example, properties like density and solubility of materials in their condensed phases. The distinguishing features of ideal and real solutions are often rationalized in terms of dominant intermolecular interactions. Typical intermolecular noncovalent bonding interactions presented at the undergraduate chemistry include van der Waals interactions, electrostatic or ionic bonds, dipole-dipole interactions, ion-dipole interactions, and the ubiquitous hydrogen bond[2].

Interestingly, there exists a plethora of noncovalent interactions that are not presented at the undergraduate level, at least not yet[3-8]. Indeed, Alkorta *et al.* recently presented a description of noncovalent interactions covering most groups of the periodic table[3]. To facilitate their recognition and discussion, these interactions are often named based on the group in which the electron deficient or Lewis acid atom participating in the interaction belongs to. Thus, the names triel, tetrel, pnictogen, chalcogen, halogen, or aerogen bonds are given to those interactions for which the Lewis acid belongs respectively to groups 13 to 18. Other names include the alkali, the alkaline earth, the regium (groups 10 and 11), and the spodium (group 12) bonds[3].

As mentioned before, an intermolecular interaction involving an atom from the boron group or group 13 is referred to as a triel bond[9-11]. One possibility for the interaction takes place when the electron deficient atom exhibits $sp^2$ hybridization in the isolated Lewis acid unit, like in the $BH_3$ molecule. Thus, in the $H_3N\cdots BH_3$ complex formation, the nitrogen atom in the Lewis base can donate a lone pair of electrons to the electron deficient $p_z$ orbital in the boron atom. This type of interaction is presented as an example of a coordinate covalent or dative bond in undergraduate chemistry[2]. Within the context of triel bonds, the $H_3N\cdots BH_3$ complex is presented as a π-hole triel bond given that the electron deficient region in the Lewis acid is perpendicular to the plane of the $BH_3$ molecule. Another possibility for the triel bond interaction can be seen in the complex of $C_5H_5B\cdots NH_3$. Here, the boron atom exhibits largely sp hybridization. The electron deficient region of the boron atoms extends in the plane of the $C_5H_5B$ molecule opposite to the line containing the boron and the carbon atoms in *para* position. This region appears with positive electrostatic potential and is termed a σ-hole[12]. Consequently, these intermolecular interactions are conveniently referred to as σ-hole triel bonds.

In this work, we examine cooperativity in σ-hole triel bonds. To this end, we selected as basic model systems the 1,4-dedihydrogenated derivatives of borazine, $B_3H_4N_3$, and azaborine, $C_4H_4BN$, respectively[13]. In this paper, we will refer to these basic 1,4-dedihydrogenated motifs simply as borazine and azaborine respectively. Accordingly, each basic motif is endowed with an electron rich region on the nitrogen atom (Lewis base site), and an electron-deficient site on the boron atom (Lewis acid site) located at the opposite side of the Lewis base site. Their amphoteric nature and relatively small sizes make them computationally convenient model systems to investigate self-aggregation and σ-hole cooperativity in triel bonds. It is worth noting that cooperativity is defined as the non-additive effects resulting from a sequence of interlinked noncovalent interactions[14]. The resulting cooperativity could be positive in which case the sum of the parts, i.e. binding energies, is less than the whole, or negative in which the sum of the parts is more than the whole. If neither positive nor negative cooperativity exists, then the interactions are deemed as simply additive interactions. Although much work on the cooperative effects in other interactions like hydrogen bonds and halogen bonds has been published, similar studies involving triel bonds remain uncommon[15-19]. Thus, the results presented here contribute to enriching our understanding of noncovalent interactions in general and that of σ-hole triel bonds in particular.

### *Computational Details*

All calculations were performed in vacuum with the ωB97XD/DGDZVP density functional method. In particular, the Gaussian 16 program was used for geometry optimizations, frequency cal-

culations, and complexes' interaction energies[20]. The AIMALL program was used to obtain the various indicators of bond strength and nature within the framework of the quantum theory of atoms in molecules, QTAIM[21-22]. For a given complex, the interaction energies were obtained by subtracting from the complex energy the sum of the energies of the isolated monomers in the geometry they have in the complex. Interaction energies were corrected for basis set superposition error (BSSE)[23].

## Results and Discussion

*Electrostatic Potentials*

The calculated electrostatic potentials of the two basic monomeric motifs are displayed in Figure 1. Here, regions of positive to negative electrostatic potential are represented in the color range from intense blue to intense red respectively. Inspection of Figure 1 reveals that both molecules show an amphoteric character with Lewis acid regions corresponding to positive electrostatic potentials (towards the blue) and Lewis base regions corresponding to negative electrostatic potentials (toward the red)[4]. It is also apparent that the Lewis acid and base regions are more intense in the borazine derivative than they are in the azaborine analogue. Moreover, the borazine derivative has regions of intense blue on the hydrogens covalently bonded to nitrogen in addition to the intense blue region on the boron atom. Based on the electrostatic potentials shown in Figure 1, it can be anticipated that attractive noncovalent interactions should occur between the Lewis base site of one molecule and the Lewis acid region of another nearby molecule, especially when the interaction is primarily electrostatic in nature[24].

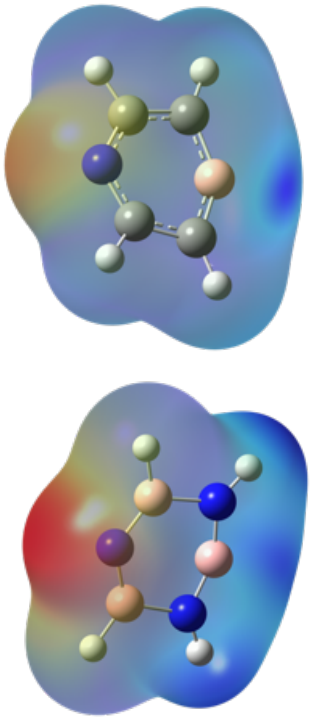

**Figure 1**. Molecular electrostatic potential maps of the optimized monomers of 1,4-dedihydro 1,4-azaborine (top) and of 1,4-dedihydro 1,4-borazine (bottom). Results displayed on the 0.001 electrons Bohr$^{-3}$ surfaces. Blue and red regions represent positive and negative molecular electrostatic potentials, respectively.

*Self-aggregation and Cooperativity*

Because the molecules chosen as model systems exhibit both Lewis acid and Lewis base regions, self-aggregation of two or more molecules is expected. For ease of discussion, the optimized geometries for the trimer complexes are displayed in Figure 2 which confirm the presence of intermolecular B···N triel bonds holding together the various monomeric units in the corresponding complexes. The point group symmetry of each of the optimized trimers is $C_2$, same symmetry as that of the optimized dimers, not shown in Figure 2 but that can be envisioned by mentally removing either terminal unit in a trimer.

Dimer formation results in large interaction energies, ΔE, for both borazine (~ -70 kcal/mol) and azaborine (~ -84 kcal/mol). The larger interaction energy for the latter is consistent with its calculated larger polarity (6.41 D) compared with that in the former (2.63 D). Evidence of cooperativity should be manifested in a number of indicators. For example, the magnitude of the average interaction energies, <ΔE>, is expected to increase upon trimer formation if positive cooperativity occurs. Table 1 shows that this is indeed the case for both trimer complexes, although the extent of the increase is larger in the borazine system (28%) than it is in its azaborine counterpart (12% increase). Dimer formation also results in a dipole moment larger than that of the corresponding monomer. Specifically, a 134% increase in the dipole moment, relative to the monomer, is seen in the dimer of the azaborine system while a corresponding 84% increase occurs in the borazine counterpart. Further evidence of cooperativity is thus provided by the rise in the

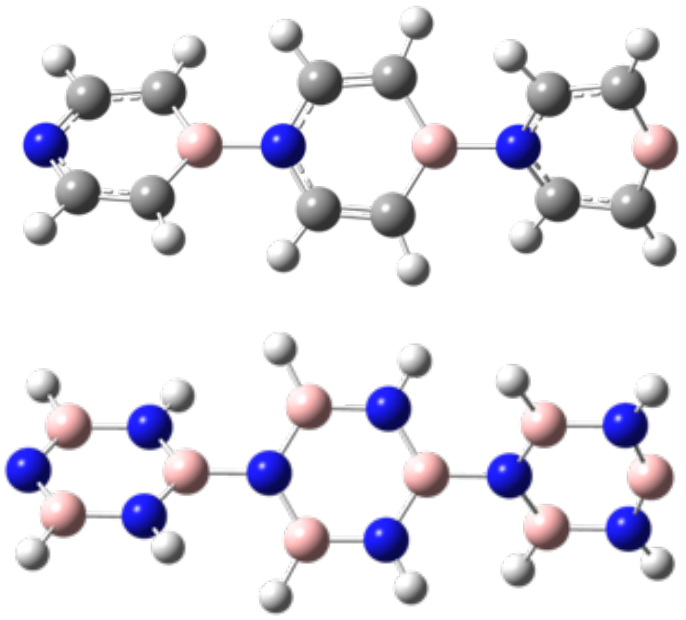

**Figure 2**. Optimized trimer complexes of 1,4-dedihydro 1,4-azaborine (top) and of 1,4-dedihydro 1,4-borazine (bottom).

**Table 1.** Average interaction energies, <ΔE>, dipole moments, <μ>, intermolecular distances, <B···N>, and stretching frequencies, <νB···N> for the dimer and trimer complexes of 1,4-dedihydrogenated azaborine and borazine model systems.

| System | <ΔE> (kcal/mol) | <μ> (D) | <B···N> (Å) | <νB···N> (cm$^{-1}$) |
|---|---|---|---|---|
| **1,4-Azaborine** | | | | |
| Dimer | -69.93 | 6.1 | 1.561 | 1160 |
| Trimer | -78.46 | 8.1 | 1.549 | 1189 |
| **1,4-Borazine** | | | | |
| Dimer | -84.45 | 11.8 | 1.554 | 1107 |
| Trimer | -108.29 | 12.5 | 1.518 | 1155 |

dipole moments in the trimers compared with those in the dimers. Again, Table 1 shows a sizeable increase of the dipole moments upon trimer formation. A geometrical parameter that is expected to provide insight on the strength of the triel bond interaction is the intermolecular B···N distance, especially when compared to the sums of their van der Waals radii (3.47)[25]. The B···N distances displayed in Table 1 for the dimers are much shorter than the sum of their van der Waals radii suggesting the existence of very strong interactions, and perhaps of a covalent character. These distances become even shorter in the trimers confirming positive cooperativity. Lastly, additional evidence of cooperative strengthening of the triel bonds is provided by the blue shift of the B···N stretching frequencies, νB-N, as can be seen in Table 1 as well.

The Quantum Theory of Atoms in Molecules (QTAIM) is a topological framework based on the electron density, ρ(*r*), derived from quantum chemical calculations[22]. QTAIM is applicable to both covalent and noncovalent interactions. It provides quantitative descriptors (ρ, $\nabla^2\rho$, energy densities) of bonding that can be used to reveal the presence, strength and nature of intermolecular interactions, as well as the extent of subtle effects like cooperativity[26,27]. Accordingly, the presence of a bond path connecting the Lewis acid (Boron) in one molecule and the Lewis base (Nitrogen) in an adjacent molecule confirms the formation of a σ-hole triel bond between the two molecules. The electron density at the bond critical point, $\rho_c$, shown in Table 2 correlates with the strength of the interactions, particularly with the corresponding average interaction energies (see Table 1). Cooperativity in the trimer is consistently indicated by a respective increase in the magnitude of $\rho_c$.

The nature of the σ-hole triel interactions as noncovalent, partly covalent, or covalent can be conveniently assessed using a combination of some pertinent QTAIM parameters. For example, the electron density at the bond critical point, $\rho_c$, tends to increase with the strength of the bonding interaction. It is also in the order of $10^{-1}$ au in the case of covalent or shared interactions, while it tends to be at least an order of magnitude smaller in the case of closed-shell non-covalent interactions. Further insight on the nature of an intermolecular interaction can be gained by considering the sign of the Laplacian of the electron density at the bond critical point, $\nabla^2\rho_c$, which if negative implies an accumulation of electron density toward the critical point (typical of a covalent bond interaction), while if positive implies an accumulation of electron density away from the critical point (typical of a noncovalent bonding interaction). It has been found that covalent bonding interactions are characterized by negative values of the total energy density, $H_c$. The magnitude of the kinetic to potential energy density ratio, $|G_c/V_c|$, is also commonly used to gauge the nature of an interaction. Specifically, when the ratio is larger than 1 the interaction is deemed to be of the closed-shell or noncovalent type. A partly covalent interaction will have the ratio between 0.5 and 1. While a pure covalent bonding will have the ratio smaller than 0.5. A partly covalent bonding interaction is also characterized by both a negative total energy density, $H_c < 0$, and a positive Laplacian, $\nabla^2\rho_c > 0$. Inspection of Table 2 leads us to conclude that the s-hole triel interactions examined in this work can all be identified as partly covalent in nature[26-30].

**Table 2.** QTAIM properties at s-hole B···N triel bond critical points in dimer and trimer complexes of 1,4-dedihydrogenated azaborine and borazine model systems: electron density, $\rho_c$, Laplacian of electron density, $\nabla^2\rho_c$, total energy density, $H_c$, and kinetic to potential energy density ratio, $|G_c/V_c|$. All quantities in atomic units.

| System | $\rho_c$ | $\nabla^2\rho_c$ | $H_c$ | $\lvert G_c/V_c\rvert$ |
|---|---|---|---|---|
| **1,4-Azaborine** | | | | |
| Dimer | 0.134 | 0.391 | -0.096 | 0.67 |
| Trimer | 0.141 | 0.364 | -0.106 | 0.65 |
| **1,4-Borazine** | | | | |
| Dimer | 0.142 | 0.262 | -0.113 | 0.61 |
| Trimer | 0.161 | 0.226 | -0.138 | 0.59 |

*Intramolecular Geometry Deformations*

Complex formation is likely to cause some changes in the intramolecular geometry of each of the monomers making up the complex relative to the noncomplexed monomer. The extent of the geometrical deformations should correlate with the strength of the intermolecular interactions[31]. Given the large interaction energies shown in Table 1, one anticipates important geometrical distortions of the monomer geometries in the dimer and in the trimer complexes. However, not all geometrical parameters are necessarily impacted to the same extent. To determine which geometrical parameters are most impacted, Table 3 displays relevant geometrical distances and angles of the azaborine monomers both in the noncomplexed one and in the complexed ones. Likewise, Table 4 displays the corresponding geometrical parameters of the borazine monomers. Figure 3 shows the optimized monomers of the azaborine and borazine derived monomers. Also shown in Figure 3 are the numerical labels used for the geometrical distances and angles displayed in Tables 3 and 4.

Inspection of Table 3 reveals that the largest geometrical changes upon azaborine dimer formation occur in the monomer acting as the triel bond donor (left monomer). For this monomer, the most important changes occur in the geometries around the Lewis acid site (boron) with an increase of about 4% in the $R_{4\text{-}9}$ distance, accompanied by a 12% widening of the $\alpha_{3\text{-}4\text{-}9}$ angle and a 15% narrowing of the $\alpha_{4\text{-}9\text{-}1}$ angle. These changes are consistent with the boron center moving from a quasi-linear geometry (*sp* hybridization) to a more trigonal planar geometry ($sp^2$ hybridization).

**Table 3.** Relevant intramolecular geometrical parameters for the monomer of 1,4-dedihydro 1,4-azaborine system in the isolated monomer and in the dimer and trimer complexes. Bond distances, R, in Å and angles, α, in degrees. See Figure 3 in text for numerical labels.

| | | Dimer | | Trimer | | |
|---|---|---|---|---|---|---|
| | Monomer | Monomer Left | Monomer Right | Monomer Left | Monomer Middle | Monomer Right |
| $R_{10\text{-}3}$ | 1.339 | 1.342 | 1.355 | 1.344 | 1.355 | 1.358 |
| $R_{3\text{-}4}$ | 1.415 | 1.395 | 1.396 | 1.393 | 1.378 | 1.393 |
| $R_{4\text{-}9}$ | 1.434 | 1.488 | 1.436 | 1.493 | 1.492 | 1.437 |
| $\alpha_{2\text{-}10\text{-}3}$ | 119.9 | 117.9 | 122.3 | 117.5 | 120.4 | 122.4 |
| $\alpha_{10\text{-}3\text{-}4}$ | 127.5 | 126.2 | 125.3 | 126.4 | 124.1 | 125.2 |
| $\alpha_{3\text{-}4\text{-}9}$ | 103.1 | 115.7 | 104.0 | 116.4 | 116.8 | 104.2 |
| $\alpha_{4\text{-}9\text{-}1}$ | 138.9 | 118.2 | 138.9 | 116.9 | 117.9 | 138.8 |

**Table 4.** Relevant intramolecular geometrical parameters for the monomer of 1,4-dedihydro 1,4-borazine system in the isolated monomer and in the dimer and trimer complexes. Bond distances, R, in Å and angles, α, in degrees. See Figure 3 in text for numerical labels.

| | | Dimer | | Trimer | | |
|---|---|---|---|---|---|---|
| | Monomer | Monomer Left | Monomer Right | Monomer Left | Monome r Middle | Monomer Right |
| $R_{10\text{-}3}$ | 1.374 | 1.386 | 1.413 | 1.390 | 1.422 | 1.423 |
| $R_{3\text{-}4}$ | 1.575 | 1.502 | 1.517 | 1.482 | 1.454 | 1.491 |
| $R_{4\text{-}9}$ | 1.335 | 1.402 | 1.336 | 1.416 | 1.412 | 1.350 |
| $\alpha_{2\text{-}10\text{-}3}$ | 128.3 | 119.6 | 126.6 | 120.3 | 120.1 | 124.6 |
| $\alpha_{10\text{-}3\text{-}4}$ | 118.3 | 121.1 | 117.8 | 120.3 | 119.3 | 118.3 |
| $\alpha_{3\text{-}4\text{-}9}$ | 99.8 | 118.4 | 104.0 | 120.3 | 121.4 | 108.3 |
| $\alpha_{4\text{-}9\text{-}1}$ | 155.4 | 121.3 | 150.0 | 118.5 | 118.7 | 142.1 |

Trimer formation brings about important changes in the geometries of the left and middle monomers while leaving the rightmost monomer geometry largely unaffected.

Inspection of Table 4 shows that the geometrical distortions occurring upon borazine dimer and trimer formation follow the same qualitative patterns seen in those with the azaborine model system. However, the extent of the geometrical deformations appears larger in the borazine complexes as can be realized in Table 5 which shows the percent changes of the monomer geometries in the dimers and trimers relative to the corresponding optimized noncomplexed monomers. These larger geometrical distortions on the borazine monomers in the complexes are in line with their relative larger interactions energies (Table 1).

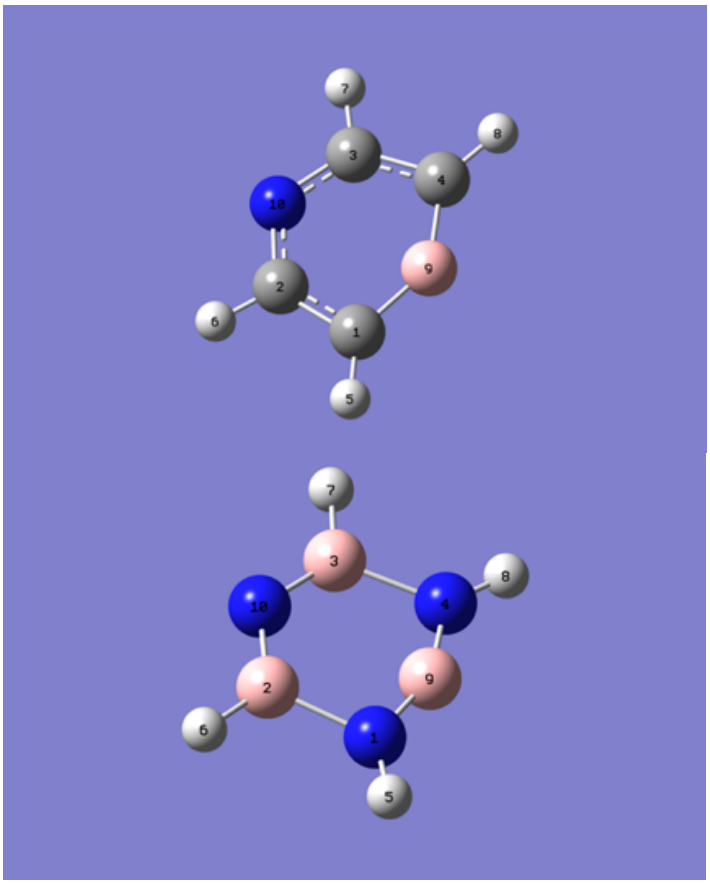

**Figure 3**. Optimized monomeric units of 1,4-dedihydro 1,4-azaborine (top) and of 1,4-dedihydro 1,4-borazine (bottom).

**Table 5.** Percent changes in the intramolecular parameters of the monomers of 1,4-dedihydro 1,4-azaborine and of 1,4-dedihydro 1,4-borazine in their dimer and trimer complexes relative to the geometries of the corresponding optimized noncomplexed monomers.

**1,4-Azaborine**

| | Dimer | | Trimer | | |
|---|---|---|---|---|---|
| | Monomer Left | Monomer Right | Monomer Left | Monomer Middle | Monomer Right |
| $R_{10\text{-}3}$ | 0% | 1% | 0% | 1% | 1% |
| $R_{3\text{-}4}$ | -1% | -1% | -2% | -3% | -2% |
| $R_{4\text{-}9}$ | 4% | 0% | 4% | 4% | 0% |
| $\alpha_{2\text{-}10\text{-}3}$ | -2% | 2% | -2% | 0% | 2% |
| $\alpha_{10\text{-}3\text{-}4}$ | -1% | -2% | -1% | -3% | -2% |
| $\alpha_{3\text{-}4\text{-}9}$ | 12% | 1% | 13% | 13% | 1% |
| $\alpha_{4\text{-}9\text{-}1}$ | -15% | 0% | -16% | -15% | 0% |

**1,4-Borazine**

| | Dimer | | Trimer | | |
|---|---|---|---|---|---|
| | Monomer Left | Monomer Right | Monomer Left | Monomer Middle | Monomer Right |
| $R_{10\text{-}3}$ | 1% | 3% | 1% | 3% | 4% |
| $R_{3\text{-}4}$ | -5% | -4% | -6% | -8% | -5% |
| $R_{4\text{-}9}$ | 5% | 0% | 6% | 6% | 1% |
| $\alpha_{2\text{-}10\text{-}3}$ | -7% | -1% | -6% | -6% | -3% |
| $\alpha_{10\text{-}3\text{-}4}$ | 2% | 0% | 2% | 1% | 0% |
| $\alpha_{3\text{-}4\text{-}9}$ | 19% | 4% | 21% | 22% | 9% |
| $\alpha_{4\text{-}9\text{-}1}$ | -22% | -4% | -24% | -24% | -9% |

*Deformation Energies and Binding Energies*

The aforementioned geometry distortions that a monomer undergoes because of complexation carry with them a corresponding energy cost known as the deformation energy, $\Delta E_{def}$. This deformation energy can be calculated for any given monomer in a complex

$$\Delta E_{def,i} = E_{complex}(i) - E_{monomer}(i) \qquad (1)$$

as shown below (Equation 1)[31].

Thus, the deformation energy for monomer *i* is obtained by subtracting the energy of the optimized noncomplexed monomer $E_{monomer}(i)$ from the energy of the same monomer but with the geometry it has in the complex, $E_{complex}(i)$. The results displayed in Table 6 for the complex systems considered in this work reveal larger deformation energies for the borazine derived complexes in agreement with their corresponding larger geometrical distortions (Table 5).

Knowing the total deformation energies (summing all monomer deformation energies in the complex) allows for the calculation of the complex binding energy, $\Delta E_{Binding}$, (Equation 2).

$$\Delta E_{Binding} = -\left(\Delta E + \sum \Delta E_{def}(i)\right) \qquad (2)$$

The binding energy thus provides a more accurate description of the complex energetic interaction by explicitly adding the total deformation energy cost to the electronic interaction energy of the complex, $\Delta E$. The calculated binding energies for the azaborine and borazine dimers are 54.72 kcal/mol and 62.06 kcal/mol. Likewise, The calculated binding energies per triel bond for the azaborine and borazine trimers are 61.35 kcal/mol and 78.10 kcal/mol. Despite the large energy costs arising from geometry distortions, the electronic binding energies remain substantially large in the dimers and with cooperative enhancements in the trimers of 12% (azaborine) and 26% (borazine) that are similar to those based solely on the electronic interaction energies.

*Summary and Outlook*

Respective dimer and trimer complexes of 1,4-dedihydro azaborine and 1,4-dedihydro borazine were investigated with the ωB97XD/DGDZVP method. For each monomer, electrostatic potential calculations show an electron rich region (Lewis base site) on the nitrogen atom opposite the boron atom which exhibits an electron deficient region or σ-hole (Lewis acid site). The attractive interactions between the Lewis acid and base sites between

**Table 6.** Deformation energies associated with the geometry distortions of the monomers of 1,4-dedihydro 1,4-azaborine and of 1,4-dedihydro 1,4-borazine in their dimer and trimer complexes relative to the energies of the corresponding optimized noncomplexed monomers. Energies are in kcal/mol and are listed for the monomers from left to right (See Figure 2).

| | Dimer | | Trimer | | |
|---|---|---|---|---|---|
| | Monomer Left | Monomer Right | Monomer Left | Monomer Middle | Monomer Right |
| 1,4-Azaborine | 13.94 | 1.27 | 15.83 | 16.87 | 1.53 |
| 1,4-Borazine | 18.63 | 3.77 | 23.85 | 28.40 | 8.14 |

properly placed adjacent molecules result in stable chain-like dimer and trimer complexes. Cooperativity effects were examined through several indicators including the interaction energies, the intermolecular distances, and the B···N vibrational stretching frequencies. Further corroboration of cooperativity was demonstrated by increases in the electron densities at the B···N bond critical points. Analyses based on the theory of atoms in molecules reveal that the noncovalent interactions are partly covalent.

Future work includes the examination of cooperativity in increasingly larger complexes up to infinite molecular chains. This will allow an estimation of cooperativity saturation and whether the nature of the triel interactions shifts from partly covalent to covalent, and if so at what complex size. Future work will also include other elements of group 13 such as aluminum. One intriguing situation is the possibility of planar complexes given the larger size of the aluminum atom which helps minimize the steric H···H interactions in adjacent molecules likely responsible for the non-planar geometries of the complexes reported in this work.

**Acknowledgement**

We send our special thanks to the Department of Chemistry and Biochemistry for its support.

**References**

1. Russo, S.; Silver, M. E. Introductory Chemistry: Atoms First. Pearson Higher Ed. Chapter 5, 2014.
2. Oxtoby, D. W.; Gillis, H. P.; Butler, L. J. Principles of Modern Chemistry. Cengage AU. Chapter 3. 2016.
3. I., Alkorta; J., Elguero; A., Frontera. Not only hydrogen bonds: other noncovalent interactions. *Crystals* **2020**, 10 (3), 180.
4. Legon, A. C.; Walker, N. R. What's in a name? 'Coinage-metal' non-covalent bonds and their definition. *Phys. Chem. Chem. Phys.* **2018**, 20(29), 19332-19338.
5. Jovanovic, D.; Mohanan, M. P.; Huber, S. M. Halogen, Chalcogen, Pnictogen, and Tetrel Bonding in Non-Covalent Organocatalysis: An Update. *Angew. Chem. Int. Ed.* **2024,** 63(31), e202404823.
6. Taylor, R. Aerogen Bond, Halogen Bond, Chalcogen Bond, Pnictogen Bond, Tetrel Bond, Triel Bond... Why So Many Names? *Cryst. Growth Des* **2024**, 24(10), 4003-4012.
7. Legon, A. C. Tetrel, pnictogen and chalcogen bonds identified in the gas phase before they had names: A systematic look at non-covalent interactions. *Phys. Chem. Chem. Phys.* **2017**, 19(23), 14884-14896.
8. Brammer, L.; Peuronen, A.; Roseveare, T. M. Halogen bonds, chalcogen bonds, pnictogen bonds, tetrel bonds and other σ-hole interactions: A snapshot of current progress. *Acta crystallogr., C Struct. chem* **2023**, 79(6).
9. Grabowski, S. J. Boron and other triel Lewis centers: From hypovalency to hypervalency. *ChemPhysChem*. 2014, 15, 2985-2993.
10. Grabowski, S. J. The nature of triel bonds, a case of B and Al centres bonded with electron rich sites. *Molecules* **2020**, 25, 2703.
11. Gao, L.; Zeng, Y.; Zhang, X.; Meng, L. Comparative studies on group III σ-hole and π-hole interactions. *J. Comput. Chem.* **2016,** 37, 1321-1327.
12. Murray, J. S. The Formation of σ-Hole Bonds: A Physical Interpretation. *Molecules* **2024**, 29(3), 600.
13. Fazen, P. J.; Burke, L.A. Theoretical Studies of Borazynes and Azaborines. *Inorg. Chem*. **2006**, 45, 2494-2500.
14. Mahadevi, A. S.; Sastry, G. N. Cooperativity in noncovalent interactions. *Chem. Rev*. **2016,** 116(5), 2775-2825.
15. Parra, R. D. Cooperative strengthening of the halogen bond in cyclic clusters of iodine monofluoride, $(IF)_n$ (n = 3–8): From a closed-shell interaction, FI… F, to a symmetric partly covalent interaction, F… I… F. *Chem. Phys. Lett.* **2022**, 803, 139825.
16. George, J.; Deringer, V. L.; Dronskowski, R. Cooperativity of halogen, chalcogen, and pnictogen bonds in infinite molecular chains by electronic structure theory. *J. Phys. Chem. A* **2014,** 118(17), 3193-3200.
17. Parra, R. D.; Grabowski, S. J. Enhancing Effects of the Cyano Group on the CX··· N Hydrogen or Halogen Bond in Complexes of X-Cyanomethanes with Trimethyl Amine: $CH_{3-n}(CN)_nX\cdots NMe_3$, (n = 0–3; X = H, Cl, Br, I). *Int. J. Mol. Sci*. **2022**, 23(19), 11289.
18. Wang, X.; Li, B.; Wang, H.; Song, Q.; Ni, Y.; Wang, H. Strong σ-hole triel-bond between $C_5H_5Tr$ (Tr=B, Al, Ga) and N-base (N-base=NCH, $NH_3$, $NC^-$): Cooperativity and solvation effects. *Chem. Phys. Lett.* **2022**, 791, 139377.
19. Karpfen, A. Linear and cyclic clusters of hydrogen cyanide and cyanoacetylene: a comparative ab initio and density functional study on cooperative hydrogen bonding. *J. Phys. Chem.* **1996**, 100(32), 13474-13486.
20. M. J. Frisch, G. W. Trucks, H. B. Schlegel et al., Gaussian 16, revision B.01. Gaussian, Inc.: Wallingford, CT, 2016.
21. Todd, A.; Keith, T. K. (2011) AIMAll (Version 11.08.23). TK Gristmill Software, Overland Park.
22. Bader, R. F. W. Atoms in Molecules: *A Quantum Theory.* **1990**, Oxford University Press, Oxford, UK.
23. Boys, S. F.; Bernardi, F. Calculation of Small Molecular Interactions by Differences of Separate Total Energies—Some Procedures with Reduced Errors. *Mol. Phys.* **1970**, 19, 553-566.
24. Murray, J. S.; Politzer, P. The electrostatic potential: an overview. Wiley *Interdiscip. Rev. Comput. Mol. Sci.* **2011,** 1(2), 153-163.
25. Bondi, A. van der Waals Volumes and Radii. *J. Phys. Chem.* **1964,** 68(3), 441–451.
26. Popelier, P. L. Non-covalent interactions from a Quantum Chemical Topology perspective. *J. Mol. Model*. **2022**, 28(9), 276.
27. Grabowski, S. J. Non-covalent interactions–QTAIM and NBO analysis. *J. Mol. Model.* **2013**, 19, 4713-4721.
28. Espinosa, E.; Alkorta, I.; Rozas, I.; Elguero J.; Molins, E. About the evaluation of the local kinetic, potential and total energy densities in closed-shell interactions. *Chem. Phys. Lett.* **2001**, 336(5–6):457–461
29. Ziółkowski, M.; Grabowski, S. J.; Leszczynski, J. Cooperativity in hydrogen-bonded interactions: ab initio and "atoms in molecules" analyses. *J Phys Chem A* **2006**, 110(20), 6514-6521.
30. Parra, R. D.; Streu, K. Hydrogen bond cooperativity in polyols: A DFT and AIM study. *Comput. Theor. Chem*. **2011**, 967, 12-18.

31. Sargent, C. T.; Kasera, R.; Glick, Z. L.; Sherrill, C. D.; Cheney, D. L. A quantitative assessment of deformation energy in intermolecular interactions: How important is it? *J. Chem. Phys.* **2023**, 58, 244106.